Symmetrical Rearrangement of the Cation-Binding Sites of Parvalbumin upon Ca^{2+}/Mg^{2+} Exchange. A Study by ^1H 2D NMR

Yves Blancuzzi,[‡] André Padilla,[*,§] Joseph Parello,[‡] and Adrien Cavé[§]

Centre National de la Recherche Scientifique URA 1111 Chimie des Médiateurs et Physico-Chimie des Interactions Biologiques, Faculté de Pharmacie, 15 Avenue Charles Flahault, 34060 Montpellier Cedex 1, France, and Centre CNRS-INSERM de Pharmacologie-Endocrinologie, Rue de la Cardonille, 34094 Montpellier Cedex, France

Received July 14, 1992; Revised Manuscript Received October 27, 1992

ABSTRACT: Two forms of parvalbumin, i.e., the fully Ca-loaded form $PaCa_2$ and the fully Mg-loaded form $PaMg_2$, are investigated by 2D ^1H NMR in solution. A detailed analysis of the resonances, which belong to residues involved in direct coordination of Ca^{2+} and Mg^{2+}, establishes that the sixth ligand, a highly conserved Glu residue at the relative position 12 in both cation-binding sites CD and EF, undergoes a conformational rearrangement through a 120° rotation of its side chain about the C^{α}–C^{β} bond with $PaMg_2$ adopting the less energetically favored g– conformation, as inferred from scalar coupling constants and dipole-dipole contacts measured on the COSY and NOESY spectra, respectively. Similarly, chemical shift effects, which selectively involve NH and $C^{\alpha}H$ resonances (as well as side-chain resonances) in both CD and EF sites, point to a symmetrical behavior of both cation-binding sites upon Ca^{2+}/Mg^{2+} exchange.

The binding of cations to parvalbumin has been intensively investigated by a variety of physicochemical methods, including atomic absorption (Donato & Martin, 1974; Nelson et al., 1977), CD[1] (Donato & Martin, 1974; White, 1988), fluorescence (Moeschler et al., 1980; White, 1988; Permyakov et al., 1980; Hutnik et al., 1990), PRE[1] and ^{25}Mg, ^{43}Ca, ^{113}Cd NMR[1] [for a review see Ribeiro et al. (1984)]. Of particular interest are the results obtained through competition with the IIA and IIB divalent cations using NMR relaxation measurements (PRE method) with the parvalbumin molecule loaded with a paramagnetic probe such as Gd^{3+} or Mn^{2+} (Cavé et al., 1979). It clearly appears that the greatest affinity is obtained for the cations Ca^{2+} and Cd^{2+} both with radii of about 0.95 Å, whereas a cation such as Sr^{2+} with a larger radius and cations with smaller radii, such as Mg^{2+} and Zn^{2+}, display reduced affinities. The ratio K_{Ca}/K_{Mg} was thus determined to be 3500, in agreement with other data using parvalbumin immobilized on a resin support (Lehky et al., 1977). This selectivity for Ca^{2+} was also observed for the single "EF hand"-like site found in the *Escherichia coli* D-galactose and D-glucose receptor (GGR) (Snyder et al., 1990). Initially, parvalbumins were described as muscle proteins, and the possible role on the calcium signal of Ca^{2+}/Mg^{2+} exchange mediated by parvalbumin was recognized very soon (Pechère et al., 1977). Since then, the investigations have been focused on the conformational aspects associated with such exchanges of two physiologically relevant cations. Spectroscopic evidence by UV, NMR, fluorescence (Birdsall et al., 1979), and, more recently, a fluorescence study (Hutnik et al., 1990) clearly suggested that the protein undergoes a conformational rearrangement upon Ca^{2+}/Mg^{2+} exchange. By comparing helix–loop–helix motifs of various Ca-binding proteins including parvalbumins, Strynadka and James (1989) suggested that the contraction of the binding loop around the smaller Mg^{2+} ion and the decrease of the coordination number from seven for Ca^{2+} to six for Mg^{2+} could involve subtle changes in the side chains of acidic coordinating groups. In their hypothesis, the invariant glutamate in position 12 which coordinates Ca^{2+} in a bidentate manner would be the key residue for the adaptation of the metal binding loop toward the binding of either Ca^{2+} or Mg^{2+}.

The crystal structure of pike p*I* 4.10 parvalbumin with its EF site loaded with Mg^{2+} has revealed that the coordination number of Ca^{2+} is changed from seven oxygen atoms [as previously determined for the crystal form $PaCa_2$ (Declercq et al., 1988)][1] to six oxygen atoms with Mg^{2+}. The main structural feature within the EF site upon Ca^{2+}/Mg^{2+} exchange appears to be the conformational rearrangement of the glutamate Glu101 side chain from the energetically favored g+ ($\chi 1 = -60°$) conformation in the Ca-loaded form to the less favored rotamer g– ($\chi 1 = +60°$) in the Mg-loaded form. In this rearrangement, the Glu101 side chain which occupies the relative position 12 (Kretsinger & Nockolds, 1973) within the amino acid sequence of the EF loop is converted from a bidentate ligand in the Ca-loaded form to a monodentate ligand in the Mg-loaded form.

The recent development of 2D and 3D NMR spectroscopy gives us the opportunity to study the structure of small proteins like parvalbumins (Padilla et al., 1988). To determine structural changes induced by the replacement of Ca^{2+} by Mg^{2+} in the CD and the EF binding sites, we have carried out NMR experiments with calcium- and magnesium-loaded pike 5.0 parvalbumin. In this paper we focus on the differences found in the two binding-site regions. Our results are discussed in the light of the X-ray structure of the pike 4.10 parvalbumin half-loaded with magnesium and demonstrate that complete Ca^{2+}/Mg^{2+} exchange involves symmetrical rearrangement of side chains in both binding sites.

MATERIALS AND METHODS

Sample Preparation. Pike parvalbumin component p*I* 5.0 is purified using the procedure of Pechère et al. (1971).

* Author to whom correspondence should be addressed.
‡ Faculté de Pharmacie.
§ Centre CNRS-INSERM de Pharmacologie-Endocrinologie.

[1] Abbreviations: CD, circular dichroism; PRE, proton relaxation enhancement; NMR, nuclear magnetic resonance; Pa, parvalbumin; TCA, trichloroacetic acid; NOESY, nuclear Overhauser effect spectroscopy; DQF-COSY, double-quantum filter correlation spectroscopy; PE-COSY, primitive exclusive correlation spectroscopy; tppi, time proportional phase incrementation; Tsp-d_4, sodium 2,2,3,3-tetradeuterio-3-(trimethylsilyl)-propionate; 1D, one dimensional; 2D, two dimensional; TNC, troponin C; CAM, calmodulin.

0006-2960/93/0432-1302$04.00/0

Following the last step in the purification, the excess of piperazine buffer was removed by gel filtration through a Sephadex G-25 column and the protein was lyophilized. At this step of the preparation, the protein contains 2.0 Ca^{2+} ions/molecule as monitored by atomic absorption spectroscopy. The $PaMg_2$ form was obtained by addition of 2.5 equiv of $MgCl_2$ to the apo-protein.

The apo-protein (Pa0) was obtained by precipitation with 3% TCA[1] (Yazawa et al., 1978). After a second purification by gel filtration through a Sephadex G-25 column, the protein was lyophilized. The evolution from the Pa(0) to the $PaMg_2$ form was monitored by the titration of the high-field $C^{\gamma}H_3$ resonance of Val 106, which presents a characteristic chemical shift for such different species as Pa0, Pa(Mg,0), or $PaMg_2$ (see Figure 1).

NMR Spectroscopy. Protein samples were dissolved in 0.5 mL of ^2H_2O or in a 90% ^1H_2O/10% ^2H_2O mixture (v/v) at a final concentration of 9.5 mM. The pH value of the solution was adjusted under pHmeter control between 6.1 and 6.5 by addition of a diluted solution (0.1 N) of deuterated ammonia or hydrochloric acid. ^2H_2O 99.8% was purchased from CEA, Saclay, France.

^1H NMR spectra were recorded on Bruker AM 600 and AMX 360 spectrometers, in the phase-sensitive mode using the TPPI[1] method (Marion & Wüthrich, 1983) and quadrature detection. Water resonance suppression was performed by low-power presaturation during the relaxation delay of about 1 s and during the mixing time of the NOESY.[1]

Prior to Fourier transformation, the data were multiplied by phase-shifted sine-bell functions. The phases shifts were $\pi/8$ and $\pi/4$ along t_1 and t_2, respectively.

NOESY spectra of $PaCa_2$ and $PaMg_2$ in H_2O solution were recorded at 600 MHz and at three temperatures (22, 32, and 42 °C). Typical acquisition parameters were 512 experiments of 4K data points and 32 scans each, with a spectral width of 6000 Hz. The mixing time was 200 ms.

DQF-COSY[1] spectra at 360 MHz in ^2H_2O were recorded at 42 °C and pH 6.5 for $PaMg_2$ and at 62 °C and pH 6.1 for $PaCa_2$. The acquisition parameters were 800 experiments of 2K data points and 64 scans each, with a spectral width of 5000 Hz.

PE-COSY[1] spectra were recorded at 360 MHz at 42 °C and pH 6.5 for $PaMg_2$ and at 62 °C and pH 6.2 for $PaCa_2$. Two sets of experiments were successively recorded with the phase-sensitive COSY pulse sequence using the detection pulse $\beta = 30°$ for the first set and $\beta = 0°$ for the second (Mueller, 1987). The data were subtracted to remove the dispersive component from the diagonal before processing. The acquisition parameters were 800 experiments of 2K data points and 32 scans each, with a spectral width of 5000 Hz.

The conventional nomenclature has been used for labeling the different protons of the amino acid spin systems (NH, $C^{\alpha}H$, $C^{\beta}H$, $C^{\beta'}H$, ...), with the chemical shift $\delta\beta > \delta\beta'$. The coupling constants $^3J_{\alpha\beta}$ and $^3J_{\alpha\beta'}$ and the sum $\sum_1 = {}^3J_{\alpha\beta} + {}^3J_{\alpha\beta'}$ of AMX spin systems can be determined, by measuring the separation of cross-peak multiplets along the F_2 dimension, from rows taken at the $C^{\beta}H$ and $C^{\beta'}H$ frequencies, in DQF-COSY and PE-COSY spectra (Griesinger et al., 1985). These experiments were processed with a digital resolution of 0.3 Hz/point.

All dihedral angles discussed in this paper are calculated from the atomic coordinates of the crystallographic structures $PaCa_2$ and PaCaMg of pike 4.10 parvalbumin (deposited with the Protein Data Bank as 1PAL and 4PAL, respectively; Declercq et al., 1991).

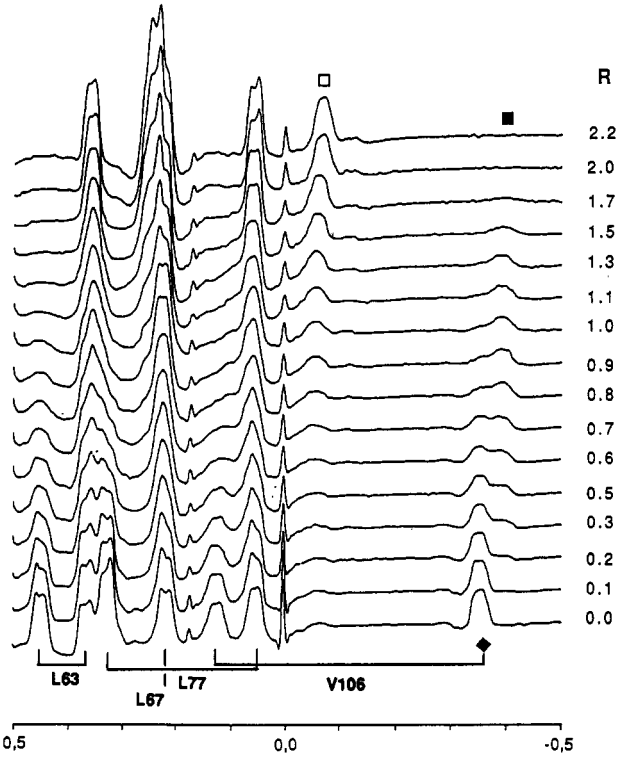

FIGURE 1: Stacked plot of the change in the upfield-shifted methyl region (+0.5/–0.5 ppm) of the 360-MHz ^1H NMR spectrum of pike parvalbumin 5.0, caused by Mg^{2+} titration of the apo-form (Pa0) of the protein, in ^2H_2O at pH 7.3 and a temperature of 20 °C. R corresponds to the molar ratio $[Mg^{2+}]/[Pa]$. Methyl resonances: (□) $C^{\gamma}H_3$ Val 106 in $PaMg_2$; (◆) $C^{\gamma}H_3$ Val 106 in Pa(0); (■) $C^{\gamma}H_3$ Val 106 in Pa(Mg,0). The methyl resonances of Val 106, Leu 63, and Leu 77 are shown by the horizontal bars. The highest field methyl resonance of Leu 67 is shown by a vertical bar.

RESULTS

Characterization of the Fully Mg-Loaded Form $PaMg_2$. As described under Materials and Methods, the fully Mg-loaded form of pike 5.0 parvalbumin was prepared from the apo-parvalbumin Pa(0) by addition of Mg^{2+} ions to the protein solution. The filling of both sites CD and EF in Pa(0) by Mg^{2+} was monitored by 1D ^1H NMR.[1] As shown in Figure 1, the upfield region of the NMR spectrum, between –0.5 and +0.5 ppm, is characterized by a series of spectral changes upon Mg^{2+} addition. The changes in intensities of the three resonances at –0.35 (black diamond), –0.4 (black square), and –0.06 ppm (open square) clearly characterize the three species Pa(0), Pa(Mg,0), and $PaMg_2$. Spectral changes are not observed upon Mg^{2+} addition above $R = 2$, indicating that the filling of both sites is complete.

2D studies of this sample at different stages of the titration clearly show that the three resonances observed between 0 and –0.5 ppm correspond to the same methyl group of the Val 106 residue. The second methyl resonance is localized between 0.12 ppm in Pa(0) and 0.35 ppm in $PaMg_2$. No stereochemical assignments of the diastereotopic *gem*-dimethyl group of Val 106 were achieved during this work. However, it is reasonable to assume that the Val 106 methyl group, which displays the greatest upfield resonance in all three molecular species during the titration, does correspond to the same methyl group (either *pro-R* or *pro-S*) in the valine side chain.

The integration of the three methyl resonance signals observed in Figure 1 is therefore reported in Figure 2. It illustrates clearly the three forms which are present during the titration by Mg^{2+}. At R about 0.9, the solution apparently

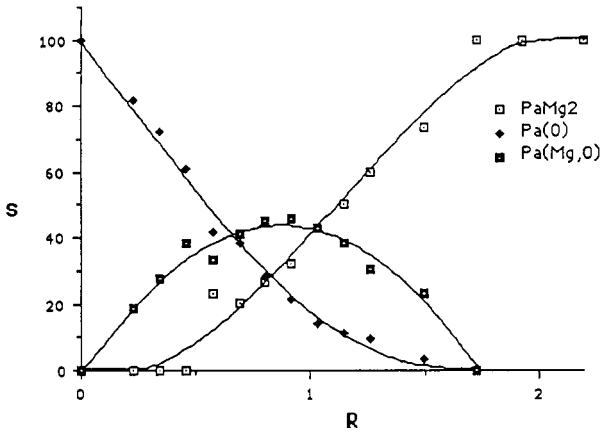

FIGURE 2: Mg^{2+} titration data of pike parvalbumin 5.0. Relative peak areas of the three upfield-shifted methyl resonances are plotted vs the Mg^{2+}/parvalbumin ratios as given in Figure 1.

corresponds to a mixture of the three parvalbumin species Pa(0), Pa(Mg,0), and $PaMg_2$. The addition of 2 equiv of Ca^{2+} to the $PaMg_2$ species restores a spectrum identical to the NMR spectrum of $PaCa_2$ after purification. This confirms that the removal of Ca^{2+} ions by TCA did not alter irreversibly the structure of the protein.

The $PaMg_2$ species obtained in the presence of a slight excess of magnesium ($R = 2.5$) was then used for establishing the sequential assignments of this novel form, through a combination of COSY and NOESY spectra at 360 and 600 MHz (Cavé et al., unpublished results), in parallel with our previous work with $PaCa_2$ (Padilla et al., 1988). These sequential assignments are used here to describe the major spectral changes which can be associated with the substitution of Ca^{2+} by Mg^{2+} in pike 5.0 parvalbumin.

Coordination of Mg^{2+} and Ca^{2+} in the CD and EF Sites. The region containing most of the $C^{\alpha}H$–$C^{\beta}H$ cross-peaks of Asp and Glu in the COSY spectra of $PaCa_2$ and $PaMg_2$ is shown in Figure 3. A comparative analysis of these cross-peaks in the PE-COSY and DQF-COSY spectra reveals the conformational features of the different side chains which participate to the direct coordination of the protein-bound cations at both sites CD and EF of parvalbumin (Figure 4).

Most of the spin systems reported in Table I correspond to AMX type (Asp, Ser, Phe residues), with the exception of the more complex systems encountered with Glu and Lys residues. All of the AMX systems [with X = $C^{\alpha}H$, M = $C^{\beta}H$, and A = $C^{\beta'}H$, following Wüthrich (1986)] can be satisfactorily analyzed in terms of their scalar coupling constants, $^3J_{\alpha\beta}$, $^3J_{\alpha\beta'}$, and $^2J_{\beta\beta'}$, as first-order systems, since the observed chemical shift differences are bigger than the strongest J coupling values (i.e., absolute value of ≈18 Hz). The Ser 55 AMX spin system is the only system which cannot be analyzed in $PaCa_2$ due to the equivalence of the $C^{\alpha}H$, $C^{\beta}H$, and $C^{\beta'}H$ resonances.

It must be noted that our analysis of the spin–spin multiplets of the AMX spin systems (and others, see below) does not include any correction for line broadening [see Wüthrich (1986)]. Therefore, the J values are not as accurate as they would be if a more elaborate treatment of the cross-peaks was used. The sum $\Sigma_1 = {}^3J_{\alpha\beta} + {}^3J_{\alpha\beta'}$, which corresponds to the full multiplet separation, can be directly measured from the $C^{\alpha}H$–$C^{\beta}H$ and $C^{\alpha}H$–$C^{\beta'}H$ cross-peaks, allowing a clear discrimination to be made between two groups of rotamers about the C^{α}–C^{β} bond ($\chi 1$ dihedral angle). The first group corresponding to the (g–) rotamer ($\chi 1 = 60°$) is characterized by Σ_1 < ca. 10 Hz, whereas the second group including the trans (t) rotamer ($\chi 1 = 180°$) and the gauche (g+) rotamer ($\chi 1 = -60°$) is characterized by Σ_1 > ca. 16 Hz [for conventions see McGregor et al. (1987)]. This distinction is based on the dependence of the ^3J constants $J_{\alpha\beta}$ and $J_{\alpha\beta'}$ on the dihedral angle $\chi 1$ according to the Karplus relation (Hyberts et al., 1987).

First Ligand at the Relative Position 1 in the CD and EF Sites. In both sites relative position 1 corresponds to an aspartic residue in all parvalbumin amino acid sequences. In pike 5.0 studied here, the side chains of Asp 51 and Asp 90 can be defined as g+ or t rotamers on the basis of Σ_1 = 16–17 Hz (see Table II). According to Wagner et al. (1987), both rotamers can be distinguished on the basis of intraresidue NOE measurements ($d_{N\beta}$ and $d_{N\beta'}$ NOEs). In the t rotamer, both Hβ and Hβ' protons are close to the NH proton at more or less the same distance ($d_{N\beta} \approx d_{N\beta'}$), whereas in the g+ rotamer the Hβ and Hβ' protons are at different distances from the NH proton. In the case of Asp 51 and Asp 90, it is observed that the strong NOE cross-peaks associated with the distances $d_{N\beta}$ and $d_{N\beta'}$ are of similar intensity, thus establishing that Asp 51 and Asp 90 adopt the t conformation in $PaCa_2$ and $PaMg_2$. This observation is in total agreement with the X-ray crystallographic data (Declercq et al., 1991), at least for the EF site.

It is noted that the NOE criterion used here for determining the rotameric state of the side chains of Asp 51 and Asp 90 is valid if one considers that the main contribution to the NOESY cross-peaks is of intraresidue origin. The two residues could be affected differently by spin diffusion since they experience a different atomic environment in the CD and EF sites. Our present conclusion concerning the t conformation of the Asp 51 and Asp 90 side chains (as well as for other aspartyl side chains) rests upon the comparison of NOE values determined at a single mixing time (see Materials and Methods) by emphasizing the similarities or the differences between the $d_{N\beta}$ and $d_{N\beta'}$ NOE intensities at a given mixing time.

As shown in Figure 5, for the trans rotamer the *pro-S* ($H^{\beta 1}$) and *pro-R* ($H^{\beta 2}$) protons in the diastereotopic $C^{\beta}H_2$ group of an aspartyl side chain are equally close to the NH proton, and therefore almost equally strong $d_{N\beta 1}$ and $d_{N\beta 2}$ NOEs are observed. The stereochemical assignment relies on the values of the $^3J_{\alpha\beta}$ coupling constant, which is large for the *pro-R* and smaller for the *pro-S* proton. Thus, for Asp 51 and Asp 90 the *pro-R* corresponds to the low-field Hβ proton resonances in Table II.

Second Ligand at the Relative Position 3 in the CD and EF Sites. As is apparent from Table II, both homologous side chains from Asp 53 and Asp 92, which occupy the relative position 3 in the CD and EF sites, respectively, clearly adopt the g– conformation in $PaCa_2$ as well as in $PaMg_2$. This observation for parvalbumin in solution is in agreement with the crystallographic data obtained with $PaCa_2$ and PaCaMg (Declercq et al., 1991). In both crystal forms, Asp 92 in the EF site adopts the g– conformation independently of the occupation of the site by Ca^{2+} or Mg^{2+}, i.e. $\chi 1 = +57°$ and $\chi 1 = +62°$ in $PaCa_2$ and PaCaMg, respectively.

Third Ligand at Position 5 in the CD and EF Sites. The relative position 5 containing the third ligand is substituted by Ser (Ser 55) in the CD site and by Asp (Asp 94) in the EF site. Due to the small chemical shift differences of the $C^{\alpha}H$ and $C^{\beta}H$ in the $PaCa_2$ form, we were not able to measure the coupling constants of Ser 55. In the $PaMg_2$ form the spin system of Ser 55 cannot be resolved in the COSY spectra. This is due to small $J_{\alpha\beta}$ coupling constants and to overlap. However, relatively strong intraresidual $d_{\alpha\beta}$ and $d_{\alpha\beta'}$ NOEs

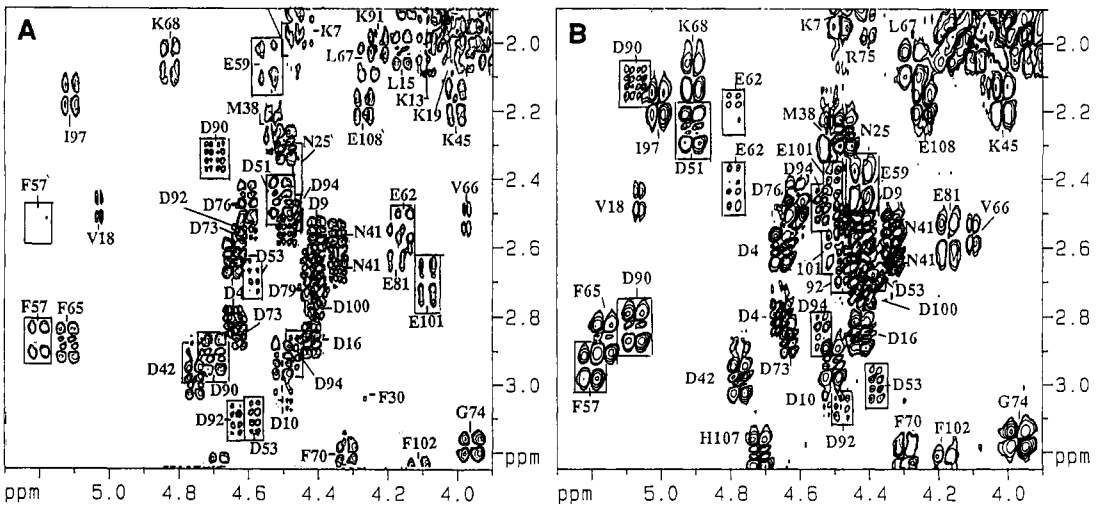

FIGURE 3: Contour plot of the $C^{\alpha}H$–$C^{\beta}H$ cross-peak region of DQF-COSY spectra for (A) $PaCa_2$ (15 mM, ^2H_2O, pH 6.1, 62 °C) and (B) $PaMg_2$ (9.5 mM, ^2H_2O, pH 6.5, 32 °C). The cross-peaks are labeled at the vertical position of the $C^{\alpha}H$ resonance with the one-letter convention. The cross-peaks of residues involved in the cation binding are D 51, D 53, F 57, E 59, and E 62 for the CD site and D 90, D 92, D 94, and E 101 for the EF site. Most of these cross-peaks are delineated by rectangles.

	X	Y	Z	-Y	-X	-Z
CD	D51 x D53	x S55	x F57CO	x E59	x x E62	
EF	D90 x D92	x D94	x K96CO	x H_2O	x x E101	
	1 2 3	4 5 6	7	8 9	10 11	12

FIGURE 4: Relative positions of the ligands in CD and EF sites according to Kretsinger and Nockolds (1973). The numbers 1–12 represent the numbering of the 12 residues of the sites, in the EF-hand motif, and the letters X, –X, Y, –Y, Z, and –Z represent the relative positions occupied by the ligands in the cation-binding sites.

can be observed. This would suggest that Ser 55 is a g– rotamer in $PaMg_2$. In the case of Asp 94 in the EF site, good agreement is again found between NMR and X-ray data. The $J_{\alpha\beta}$ coupling constants and the NOE criteria (two strong $d_{\alpha\beta}$ NOE cross-peaks) are consistent with a g– conformation for Asp 94, for which no difference can be noted between Ca^{2+} and Mg^{2+} forms.

Fourth Ligand at Position 7 in the CD and EF Sites. The homologous position 7 in the CD site is invariably substituted by an aromatic residue (Phe or Tyr) coordinated to the cation through its carbonyl group. Both $PaCa_2$ and $PaMg_2$ forms of pike 5.0 present a vicinal coupling constant $J_{\alpha N}$ = ca. 9.4–9.5 Hz, which probably corresponds to a ϕ angle of ca. –120° (as inferred from a Karplus plot determined with BPTI; Wüthrich, 1986). This value can be compared with –137° ($PaCa_2$ pike 4.10), –129° (PaCaMg pike 4.10), and –138° (shark parvalbumin $PaCa_2$; Roquet et al., 1992). Such an observation in solution and in the crystal points to a strict conservation of the conformation of the main chain in the CD loop, corresponding to its involvement in direct cation binding. The data given in Table II suggest a g+ or t rotamer for the side chain of Phe 57 in $PaMg_2$. Dynamical processes such as rotation of the aromatic ring about the C^{β}–C^{γ} bond may interfere with the NOE interpretation. This is the case with Phe 57, where we observed small intra-$d_{N\beta}$ NOEs compared with the other $d_{N\beta}$ listed in Table II.

The relative position 7 in the EF site of pike 5.0 parvalbumin is substituted by Lys. The Lys side chain must be exposed to the solvent, and this residue coordinates to the cation through its carbonyl group. A strong coupling constant ($J_{\alpha N}$ = ca. 9–10 Hz) is also observed as for Phe 57 and is consistent with the presence of this residue in a short β strand linking the two sites CD and EF. The $C^{\alpha}H$–$C^{\beta}H$ cross-peaks of Lys 96 are hardly observed both in $PaCa_2$ and in $PaMg_2$ due to overlap with stronger neighboring cross-peaks. However Σ_1 values of about 10.7 Hz for $PaMg_2$ and 13.3 Hz for $PaCa_2$ can be measured. The Σ_1 value observed for $PaMg_2$ lies at the upper limit for the g– $\chi 1$ conformation (≈10 Hz), and the Σ_1 value observed for $PaCa_2$ is below the limit for the g+/t rotamer (≈16 Hz). This could be due to the occurrence of a dynamical process with rapid interchange (on the NMR time scale) of different conformational states along the lysyl side chain, instead of a unique and well-defined $\chi 1$ rotamer. It is interesting to note that the residue at position 7 in the EF site of pike 4.10 parvalbumin (a methionine residue) undergoes a g+ to g– conformational change, when Ca^{2+} is substituted by Mg^{2+} in the EF site, as inferred from the X-ray crystallographic data with the $PaCa_2$ and PaCaMg forms (Declercq et al., 1991). The present NMR data could correspond to such a conformational rearrangement of the Lys side chain, the g– rotamer being preponderant for $PaMg_2$ and the g+ (or t) for $PaCa_2$.

It clearly appears that the substitution of Ca^{2+} by Mg^{2+} in the EF site of pike 4.10 parvalbumin is accompanied by a shortening of about 0.4 Å of the intercationic distance between sites CD and EF. Such a compaction effect of the parvalbumin 3D structure might be responsible for the g+ to g– rearrangement observed with Met 96.

Fifth Ligand at the Relative Position 9 in the CD and EF Sites. Only the CD loop is concerned since the Gly 98 residue at position 9 in the EF loop does not contribute to the coordination and the –X axis remains accessible to the solvent. The side chain of Glu 59 contributes directly to ion coordination in the CD site. According to Strynadka and James (1989), the length of the glutamyl side chain is well adapted to ion coordination in this –X position, contrary to the shorter side chain, such as Asp residue in this position, which is not able to coordinate directly to the ion. For Glu 59, only one $C^{\alpha}H$-$C^{\beta}H$ cross-peak, can be observed in the COSY spectra of $PaCa_2$ and $PaMg_2$, and Σ_1 has been measured in the PE-COSY spectra of both species. From the value of Σ_1 = 16.4 Hz and the weak $d_{N\beta}$ and the strong $d_{N\beta'}$ NOEs observed in the 3D HOHAHA–NOE experiment (unpublished results), a g+ rotamer is expected for Glu 59 in $PaCa_2$. This is in agreement with the X-ray data. For the $PaMg_2$, in the absence of any clearly observable $d_{N\beta}$ and $d_{N\beta'}$ NOEs, the Σ_1 value of 16.4 Hz only suggests the presence of a g+ or t rotamer.

Table I: ^{1}H Chemical Shifts for the Residues Involved in the Calcium or Magnesium Binding[a]

	$PaCa_2$				$PaMg_2$			
residue	NH	$C^\alpha H$	$C^\beta H$	$C^\gamma H$	NH	$C^\alpha H$	$C^\beta H$	$C^\gamma H$
D 51	7.50	4.51	2.44, 1.40		7.56	4.92	2.26, 1.24	
D 53	8.17	4.62	3.11, 2.70		9.84	4.40	3.02, 2.66	
S 55	8.88	4.35	4.30	8.97 (OH)	9.04	4.38	4.19, 3.90	11.16 (OH)
F 57	8.00	5.26	2.86, 2.47		8.26	5.24	2.99, 2.36	
E 59	7.77	4.55	2.29, 2.05	2.64, 1.90	8.10	4.44	2.47, 2.20	2.58
E 62	6.90	4.15	2.58	2.47, 2.01	6.92	4.82	2.44, 2.17	2.60, 2.32
D 90	8.49	4.71	2.90, 2.32		8.52	5.09	2.83, 2.11	
D 92	8.59	4.67	3.12, 2.65		10.01	4.49	3.08, 2.68	
D 94	8.40	4.49	2.90, 2.48		8.65	4.56	2.86, 2.49	
K 96	8.01	4.82	1.67, 1.54		7.91	4.76	1.71, 1.42	
E 101	7.72	4.12	2.70	2.49, 2.43	8.00	4.53	2.61, 2.39	

[a] The chemical shifts are given according to internal reference Tsp-d_4 (see Materials and Methods). T = 22 °C; pH 6.5.

Table II: $^3J_{\alpha\beta}$ Coupling Constants (COSY in ^2H_2O) and Intraresidue $d_{N\beta}$ NOEs for the CD and EF Binding Sites for the Residues Involved in the Binding of the Cations

		$PaMg_2$							$PaCa_2$						
rel pos[a]	residue	$J_{\alpha\beta}$[b]	$J_{\alpha\beta'}$	Σ_1	$d_{N\beta}$[c]	$d_{N\beta'}$	NMR rot.[d]	XR rot.	$J_{\alpha\beta}$	$J_{\alpha\beta'}$	Σ_1	$d_{N\beta}$	$d_{N\beta'}$	NMR rot.	XR rot.
CD 1	D 51	11.3	4.8	17.2	+	+	t		11.5	4.9	16.5	+	+	t	t
3	D 53		3.9	9.2	–	+	g–		3.6	3.1	8.2	–	+	g–	g–
5	S 55														g–
7	F 57	10.5	3.7	16.1			g+/t		11.3	3.5	16.5			g+/t	g+
9	E 59			16.4			g+/t				16.6	–	+	g+	g+
12	E 62	4.0	3.5	8.5			g–				14.1			g+/t	g+
EF 1	D 90	11.9	5.1	16.5	+	+	t	t	12.2	4.8	17.0	+	+	t	t
3	D 92			8.2*	–	+	g–	g–		4.0	8.9	–	+	g–	g–
5	D 94	4.3	3.4	9.6			g–	g–	4.5	3.6	8.7			g–	g–
7	K 96			10.7*				g–			13.3				g+
9	w														
12	E 101		4.6	9.1			g–	g–			14.1			g+/t	g+

[a] The relative positions of the ligands are given according to Kretsinger and Nockolds (1973). [b] The $^3J_{\alpha\beta}$ coupling constants were determined by measuring the separation of the lines (see Materials and Methods), and $\Sigma_1 = J_{\alpha\beta} + J_{\alpha\beta'}$. The digital resolution for PE-COSY and DQF-COSY was 0.3 Hz/point in F_2 direction. An asterisk shows the values measured from the DQF-COSY spectra. Hβ and Hβ′ are localized, respectively, at low and high field. [c] The relative intensities between $d_{\beta N}$ NOEs were obtained from integration of the corresponding cross-peak in several NOESY spectra for $PaCa_2$ and $PaMg_2$ and are reported as + for strong NOE and – for weak NOE. [d] The rotamers were determined as in Wagner et al. (1987) and are reported in the column NMR rot. and are given according to the convention of McGregor and Islam (1987). The rotamers measured from the X-ray structure of pike 4.10 are given with the same convention in the column XR rot.

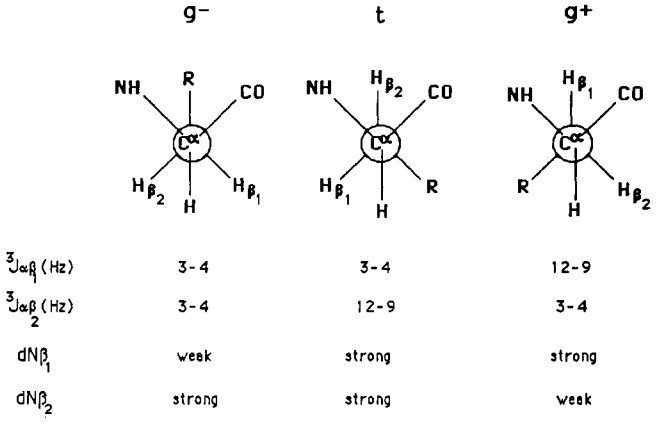

FIGURE 5: Schematic drawings of the three rotamers shown with the Newman convention. Estimates of the $^3J_{\alpha\beta}$ coupling constants and the $d_{N\beta}$ NOE intensities are given. The *pro-R* and the *pro-S* $C^\beta H$ protons correspond to $H\beta_1$ and $H\beta_2$, respectively, in the case of Lys, Arg, Glu, Gln, and Leu amino acids and correspond to the reverse order $H\beta_2$ and $H\beta_1$, respectively, in the case of Asp, Asn, Ser, Cys, Met, Phe, His, Tyr, and Trp amino acids.

Sixth Ligand at the Relative Position 12 in the CD and EF Sites. The conformational analysis of the remaining ligands, i.e., Glu 62 in the Cd site on one hand and Glu 101 in the EF site on the other hand, also rests upon the determination of the $J_{\alpha\beta}$ and $J_{\alpha\beta'}$ constants from the corresponding cross-peaks in the PE-COSY spectra. Although a glutamic residue involves a five-spin system, the analysis can be carried out in the first-order approximation since the $C^\beta H_2$ and $C^\gamma H_2$ chemical shifts are sufficiently distinct (see Table I) so that no second-order effects (virtual coupling) can be expected to occur [for an example of virtual coupling in a $CH–CH_2–CH_2$ system, see Parello et al. (1968)]. The corresponding coupling constants are listed in Table II.

A remarkable feature is that both glutamyl side chains at position 12 in the CD and EF sites, i.e., Glu 62 and Glu 101, respectively, undergo well-defined conformational changes upon Ca^{2+}/Mg^{2+} exchange. For Glu 62 and Glu 101 in the $PaMg_2$ form, we observe Σ_1 values of 8.5 and 9.1 Hz, respectively, which can be interpreted as arising from a g– rotamer in both glutamyl side chains. The conformations of Glu 62 and Glu 101 in $PaCa_2$ correspond to either a distorted g+ or t conformer on the basis of Σ_1 = 14.1 Hz. When the EF site of the parvalbumin is substituted by Mg^{2+} instead of Ca^{2+} as in PaCaMg (Declercq et al., 1991), a g– rotamer ($\chi 1 = 62°$) is observed for the side chain of Glu 101, whereas the side chain of Glu 62 remains g+ as in $PaCa_2$. The lower values of Σ_1 = 14.1 Hz observed for glutamic residues in comparison with the higher value observed for aspartic residues suggest the presence of a distorted g+ or t rotamer. Indeed, if the atomic arrangement about the $C^\alpha–C^\beta$ bond were significantly distorted from its staggered conformation (see Figure 5), it could be anticipated that Σ_1 would decrease significantly. The presence of similar constants of about 7

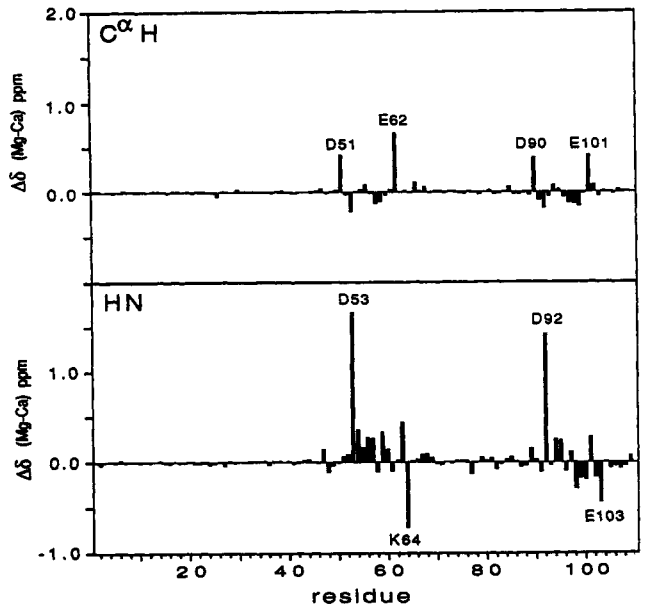

FIGURE 6: Plots of the differences of the chemical shifts, $\Delta\delta$(Mg–Ca) for the NH and the $C^{\alpha}H$ proton resonances of all residues of the protein. The chemical shift values were obtained by the analysis of NOESY spectra recorded at the same temperature (22 °C) and pH (6.5) for $PaCa_2$ and $PaMg_2$ and are calibrated using Tsp-d_4 as internal reference.

Hz for $J_{\alpha\beta}$ and $J_{\alpha\beta'}$ could also correspond to averaged values over a population of several conformations rapidly interconverting on the NMR time scale. However, this hypothesis cannot be verified as the $C^{\beta}H$ and $C^{\beta'}H$ resonances of Glu 62 residues as well as those of Glu 101 are equivalent in the NMR spectrum of the $PaCa_2$ form (see Figure 3), so no precise measurement can be performed on the cross-peaks. In the crystal form a single $\chi 1$ conformation, i.e., g+, has been described for Glu 62. However, it is an open question whether the side chain of Glu 62 in the CD site is subject to a conformational equilibrium or corresponds to a unique g+/t distorted conformation, in solution and in the crystal structure of $PaCa_2$. Such a deviation from standard values is not observed in the case of Glu 62 and Glu 101 in $PaMg_2$, where a well-defined g– conformer is determined to be present and where two distinct resonances are observed for $C^{\beta}H$ and $C^{\beta'}H$.

Owing to the fact that the coordination of the central ion in the CD and EF sites of parvalbumin imposes well-defined constraints on the direct ligands (pentagonal bipyramid for calcium and octahedron for magnesium), a dynamic state is to be considered seriously and will certainly require a more detailed analysis by NMR. Moreover, changes of the $\chi 2$ angle of the glutamyl side chains would be detected by measuring $^3J_{\beta\gamma}$ coupling constants. However, we could not perform the analysis of the $C^{\beta}H$–$C^{\gamma}H$ cross-peaks of Glu 62 and Glu 101 due to overlap.

Chemical Shift Effects upon Ca/Mg Exchange of Residues in the CD and EF Cation-Binding Loops. Finally, our conclusion that Ca^{2+}/Mg^{2+} exchange corresponds to a structurally symmetrical process for both sites CD and EF in parvalbumin is substantiated by the observation of the chemical shifts affecting the main-chain NH and $C^{\alpha}H$ resonances from the residues within the CD and EF loops upon substitution of Ca^{2+} by Mg^{2+}.

As shown in Figure 6, both homologous residues Asp 53 and Asp 92, which occupy the second position along the +Y direction in both coordination shells CD and EF, experience a similar downfield variation for their NH resonances of about 1.5 ppm upon substitution of Ca^{2+} by Mg^{2+}. A complete pattern of $\Delta\delta$ (NH) variations for the residues encompassing the CD and EF loops is presented in Figure 6. Again, a similar shift, but upfield (ca. –0.5 ppm), is observed for the NH resonances of both homologous residues Lys 64 and Glu 103. A comparison of all the other NH resonances in the CD and EF loops indicates that the chemical shift effects are of smaller magnitude (not exceeding ±0.3 ppm) and do not correlate in a symmetrical manner between the two sites. The behavior of the $C^{\alpha}H$ resonances from the residues in the CD and EF loops upon Ca^{2+}/Mg^{2+} exchange again emphasizes the symmetrical behavior observed with the NH resonances. The chemical shift variations of the $C^{\alpha}H$ resonances are of reduced amplitude in comparison with the NH resonances. However, both homologous residues Asp 51 and Asp 90 (occupying the first position along the +X direction in both coordination shells CD and EF) experience similar downfield shifts (ca. +0.4 ppm) of their $C^{\alpha}H$ resonances upon substitution of Ca^{2+} by Mg^{2+}. This is also the case for both homologous residues Glu 62 and Glu 101 (downfield shifts of +0.75 and +0.45 ppm, respectively), which act as the sixth ligands along the –Z direction of the coordination shells CD and EF.

A detailed account of the observed chemical shift variations on the NMR spectra of $PaCa_2$ and $PaMg_2$ is beyond the scope of the present paper. However, it must be noted that all of the significant variations which occur for the NH and $C^{\alpha}H$ resonances originate from residues located within the CD and EF cation-binding loops. Particularly interesting in this respect is the observation that the largest chemical shift variations observed arise for residues having their side chains directly involved in cation coordination. The Glu 62 $C^{\beta}H_2$ resonances (chemically equivalent) in $PaCa_2$ at 2.58 ppm are shifted upfield by 0.14 and 0.40 ppm in $PaMg_2$ (at 2.44 and 2.17 ppm), respectively (see Table I). Similarly, the chemically equivalent Glu 101 $C^{\beta}H_2$ resonances at 2.7 ppm in $PaCa_2$ are shifted upfield by 0.1 and 0.3 ppm in $PaMg_2$ and give rise to two nonequivalent resonances $C^{\beta}H$ and $C^{\beta'}H$ at 2.61 and 2.39 ppm, respectively (see Table I). The $C^{\beta}H_2$ resonances of Asp 51 and Asp 90 are also slightly shifted upfield (by 0.1–0.2 ppm) upon substitution of Ca^{2+} by Mg^{2+}. These variations remain small by reference to the large and characteristic inequivalence of the $C^{\beta}H$ proton resonances (about 1 ppm for Asp 51 and about 0.6–0.7 ppm for Asp 90).

Most of our observations can probably be explained as due to the variations in the position of the charged groups (including the cation itself) in the parvalbumin 3D structure upon Ca^{2+}/Mg^{2+} exchange. The proximity between the carboxylic group in an Asp residue with its $C^{\alpha}H$ in the t rotamer and or with its NH amide proton in the g– rotamer (see Figure 5) could partly account for the chemical shift differences observed in Asp 51, Asp 90 ($C^{\alpha}H$) and in Asp 53, Asp 92 (NH). In contrast, the smaller difference for the NH chemical shift of Asp 94 could correspond to small geometrical changes in the environment of this residue. It is well established that NMR chemical shift values are determined by a relatively large number of individual contributions (Pople et al., 1959), so that quantitative predictions are usually poor, except for selected effects such as the relatively strong ring current effects (Perkins & Wüthrich, 1979). The observation upon Ca^{2+}/Mg^{2+} exchange of similar chemical shift effects for resonances originating from homologous positions in the CD and EF sites clearly suggests that the substitution of Ca^{2+} by Mg^{2+} and vice versa in both primary sites of parvalbumin are charac-

terized by a symmetrical conformational behavior in agreement with the local symmetry (approximate twofold axis) of the double "EF hand" motif in the protein. In addition, if we take into consideration the fact that the ligand at the relative position 12 in the CD and EF loops (Glu 62 and Glu 101, respectively) adopts the same energetically unfavored g– conformation upon substitution by Mg^{2+}, we may conclude that both sites CD and EF undergo very similar structural rearrangements upon Ca^{2+}/Mg^{2+} exchange.

Obviously, perfect symmetry cannot be expected between both cation-binding sites CD and EF in parvalbumin since the substitution of their homologous positions differs markedly in the chemical nature of the corresponding side chains. Among the residues directly interacting with the central cation, a marked difference is observed at position 5 in both loops, with Ser 55 in the CD site and Asp 94 in the EF site. The interchange of dipolar ligands for charged carboxylate ligands between both ligands is likely to explain the systematic differences observed for the ^{113}Cd resonances associated with the Cd-loaded parvalbumin $PaCd_2$ (Cavé et al., 1982). Whereas Phe appears at the relative position 7 of the CD site, the same position in the EF site is substituted by Lys. Since both side chains are included in the folding of the protein, the variety of interresidue contacts in the 3D structure may impose different constraints for each site, thus interfering with the symmetrical arrangement of both sites.

DISCUSSION

In conclusion, our 2D ^1H NMR study of two forms of parvalbumin in solution, i.e., $PaCa_2$ and $PaMg_2$, clearly establishes the crucial role of the sixth ligand on the binding of cations of both the CD and EF sites. The sixth ligand at the relative position 12 of the "EF hand" loop invariably corresponds to Glu in both sites of parvalbumin. In the $PaMg_2$ form, the glutamyl side chain adopts, in both sites CD and EF, the energetically unfavored g– $\chi 1$ rotamer, whereas in the $PaCa_2$ form the glutamyl chain adopts the energetically favored g+ conformation. This observation by NMR for solution is in agreement with a previous result by X-ray crystallography concerning the organization of the EF site occupied by Ca^{2+} or Mg^{2+}. The NMR study clearly establishes for the first time that the homologous glutamyl side chain at position 12 in the CD site adopts the same g– conformation when Mg^{2+} occupies the site. The present NMR study shows that both sites CD and EF behave in a symmetrical manner upon Ca^{2+}/Mg^{2+} exchange. Such a behavior is substantiated by the observation of similar chemical shift effects for the ^1H NMR resonances from residues occupying homologous positions in the CD and EF sites. These chemical shifts are explained by electric field effects originating from charged groups, which are displaced, although slightly, upon Ca^{2+}/Mg^{2+} exchange at the level of both coordination spheres CD and EF. The local rearrangement of charged groups within the binding loop may strongly affect the chemical shifts, as is the case for the OH resonance of Ser 55 in $PaCa_2$ and $PaMg_2$ (see Table I). Finally, we have observed selective chemical shift effects involving methyl resonances of a few nonpolar residues within the hydrophobic core of parvalbumin, in particular Leu 63. This clearly establishes a link between the local rearrangements at the level of the cation-binding sites CD and EF themselves and the overall structural organization of the protein upon Ca^{2+}/Mg^{2+} exchange.

Other proteins that belong to the calcium superfamily, like TNC[1] and CAM,[1] possess high-affinity sites able to bind calcium and magnesium with different affinity constants. The functions of these sites are still not well-defined, and the usual hypothesis is that they might be structural domains. The TNC and CAM proteins possess structure homology with parvalbumins, and it has been demonstrated that large differences in their structure occur during the binding of calcium. Studies realized on TNC (Herzberg & James, 1988), CAM (Babu et al., 1988), and parvalbumin (Declercq et al., 1991) have shown the existence of constant structural features between these proteins. Thus, it appears as an important challenge to verify whether the model given by parvalbumin during the Ca^{2+}/Mg^{2+} exchange can be transposed to the cases of other proteins, such as TNC and CAM, for which the role of the Ca^{2+}/Mg^{2+} high-affinity binding sites remains unclear.

ACKNOWLEDGMENT

We thank Gérard Etienne for preparing the samples of parvalbumin and the Laboratoire de RMN de l'Ecole Polytechnique (Palaiseau) for the use of the 600-MHz spectrometer.

REFERENCES

Babu, Y. S., Bugg, C. E., & Cook, W. J. (1988) *J. Mol. Biol. 204*, 191–204.

Birdsall, W. J., Levine, B. A., Williams, R. J. P., Demaille, J. G., Haiech, J., & Pechère, J. P. (1979) *Biochimie 61*, 741–750.

Cavé, A., & Parello, J. (1981) in *Les Houches, session XXXIII, 1979, Membranes et communication intracellulaire* (Balians et al., Eds.) pp 197–227, North-Holland Publishing, Amsterdam.

Cavé, A., Daures, M. F., Parello, J., Saint-Yves, A., & Sempéré, R. (1979) *Biochimie 61*, 755–765.

Cavé, A., Saint-Yves, A., Parello, J., Swärd, M., Thulin, E., & Lindman, B. (1982) *Mol. Cell. Biochem. 44*, 161–172.

Declercq, J. P., Tinant, B., Parello, J., Etienne, G., & Huber, R. (1988) *J. Mol. Biol. 202*, 349–353.

Declercq, J. P., Tinant, B., Parello, J., & Rambaud, J. (1991) *J. Mol. Biol. 220*, 1017–1039.

Donato, H., Jr., & Martin, B. R. (1974) *Biochemistry 13*, 4575–4579.

Einspahr, H., & Bugg, C. E. (1981) *Acta Crystallogr. Sect. B 37*, 1044–1052.

Grieisinger, C., Sørensen, O. W., & Ernst, R. R. (1985) *J. Am. Chem. Soc. 107*, 6394–6396.

Herzberg, O., & James, M. N. G. (1988) *J. Mol. Biol. 203*, 761–779.

Hutnik, C. M. L., MacManus, J. P., & Szabo, A. G. (1990) *Biochemistry 29*, 7318–7328.

Hyberts, S. G., Märki, W., & Wagner, G. (1987) *Eur. J. Biochem. 166*, 625–635.

Kretsinger, R. H., & Nockolds, C. E. (1973) *J. Biol. Chem. 248*, 3313–3326.

Lehky, P., Comte, M., Fisher, E. H., & Stein, E. A. (1977) *Anal. Biochem. 82*, 158–169.

Marion, D., & Wüthrich, K. (1983) *Biochem. Biophys. Res. Commun. 113*, 967–974.

McGregore, M. J., Islam, S. A., & Sternberg, M. J. E. (1987) *J. Mol. Biol. 198*, 295–310.

Moeschler, H. J., Shaer, J. J., & Cox, J. A. (1980) *Eur. J. Biochem. 11*, 73–78.

Mueller, L. (1987) *J. Magn. Reson. 72*, 191–196.

Nelson, D. J., Miller, T. L., & Martin, B. R. (1977) *Bioinorg. Chem. 7*, 325–334.

Padilla, A., Cavé, A., & Parello, J. (1988) *J. Mol. Biol. 224*, 995–1017.

Parello, J., Bertrand, C., & Bedos, C. (1968) *Bull. Soc. Chim. Fr.* 5034–5035.

Parello, J., Cavé, A., Puigdomenech, P., Maury, C., Capony, J. P., & Pechère, J. F. (1974) *Biochimie 56*, 61–76.

Parello, J., Cavé, A., Cusack, S., Blancuzzi, Y., & Padilla, A. (1991) presented at the European Research Conference 1991, Research Conference on NMR in Molecular Biology, Heemskerk, Netherlands, May 20–24, 1991.

Pechère, J. F., Capony, J. P., & Ryden, L. (1971) *Eur. J. Biochem. 23*, 421–428.

Pechère, J. F., Derancourt, J., & Haiech, J. (1977) *FEBS Lett. 75*, 111–114.

Perkins, J. P., & Wüthrich, K. (1979) *Biochim. Biophys. Acta 576*, 409–423.

Permyakov, Y. E. A., Yarmolenko, V. V., Yemel'yanenko, V. I., Burstein, E. A., Gerday, C., & Closset, J. (1980) *Biophysics 25*, 430–436.

Pople, J. A., Schneider, W. G., & Bernstein, H. J. (1959) in *High-resolution Nuclear Magnetic Resonance*, McGraw-Hill, New York.

Ribeiro, A., Parello, J., & Jardetzky, O. (1984) *Prog. Biophys. Mol. Biol. 43*, 95–160.

Roquet, F., Declercq, J. P., Tinant, B., Rambaud, J., & Parello, J. (1992) *J. Mol. Biol. 223*, 705–720.

Snyder, E. E., Buoscio, B. W., & Falke, J. (1990) *Biochemistry 29*, 3937–3943.

Strynadka, N., & James, M. (1989) *Annu. Rev. Biochem. 58*, 951–998.

Wagner, G., Braun, W., Havel, T., Schaumann, T., Go, N., & Wüthrich, K. (1987) *J. Mol. Biol. 196*, 611–639.

White, D. H. (1988) *Biochemistry 27*, 3357–3365.

Wüthrich, K. (1986) *NMR of Proteins and Nucleic Acids*, p 79, Wiley, New York.

Yazawa, M., Kuwayama, H., & Yagi, K. (1978) *J. Biochem. 84*, 1253–1258.